

AD 20890

ELECTRONIC MATERIALS DIVISION

360 Sierra Madre Villa, Pasadena, California 91109 (213) 796-9381

Development of GeAs Infrared Window Materials

Contract No. N00014-75-C-2112

Sponsored by Advanced Research Projects Agency

ARPA Order No. 485

TECHNICAL SUMMARY REPORT

December 1975

Office of Naval Research, Physics Branch
Arlington, Virginia 22207



Reproduced by
**NATIONAL TECHNICAL
INFORMATION SERVICE**
Springfield, Va. 22151



BELL & HOWELL

48

**BEST
AVAILABLE COPY**

DEVELOPMENT OF GaAs INFRARED WINDOW MATERIAL

Technical Summary Report

Contract No. N00014-70-C-0132

Prepared by

Alan G. Thompson

Approved by


Robert K. Willardson, General Manager

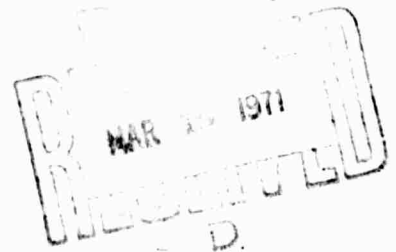
BELL & HOWELL ELECTRONIC MATERIALS DIVISION
PASADENA, CALIFORNIA 91109

December, 1970



Submitted to

OFFICE OF NAVAL RESEARCH
PHYSICS BRANCH
ARLINGTON, VIRGINIA 22217



This document has been approved for public release and sale; its distribution is unlimited.

Reproduction in whole or in part is permitted for any purpose of the United States Government.

This research is part of Project DEFENDER under the joint sponsorship of the Advanced Research Projects Agency, the Office of Naval Research, and the Department of Defense.

ABSTRACT

The choice of a window material suitable for high power CO₂ lasers emitting at 10.6 microns is discussed. Gallium arsenide was chosen as the primary candidate with gallium antimonide being the object of a subsidiary investigation. The preparation of GaAs is discussed at length. The physical, electrical and optical properties of GaAs are also discussed with particular reference to the high-resistivity form which is necessary to reduce free-carrier absorption at 10.6 microns to an acceptable level. The method used to measure the optical absorption coefficient is a calorimetric one making use of a low power CO₂ laser. The variation of the optical absorption coefficient with impurities, different dopants and resistivity is examined. An attempt was made to prepare high-resistivity GaSb, but this work is not yet complete. The preparation of larger diameter windows is described, with 3" being shown to be attainable with present technology.

CONTENTS

	<u>Page</u>
1. INTRODUCTION	1
2. CRYSTAL GROWTH	4
2.1 GaAs - Sealed System Technique	4
2.2 GaAs - Liquid Encapsulation Techniques	7
2.3 GaSb - Growth Techniques	10
3. PHYSICAL AND ELECTRICAL PROPERTIES	12
3.1 Semi-insulating GaAs	12
3.2 Physical Properties of GaAs	13
3.3 Impurities in GaAs	13
3.4 Electrical Properties of Semi-insulating GaAs	18
3.5 Properties of GaSb	19
4. OPTICAL PROPERTIES	23
4.1 Optical Properties of GaAs	23
4.2 Measurement of Optical Absorption Coefficient	25
4.3 Results for GaAs	28
4.4 Optical Properties of GaSb	32
5. LARGE DIAMETER GaAs	33
5.1 Material Preparation	33
5.2 Results	35

	<u>Page</u>
6. CONCLUSIONS AND FUTURE WORK	37
7. ACKNOWLEDGMENTS	38
8. REFERENCES	39

FIGURES

<u>Figure No.</u>		<u>Page</u>
1	Diagram of Apparatus Used for Pulling Crystals by the Sealed Czochralski Technique	5
2	A Typical {111} Cr-doped GaAs Single Crystal Ingot	6
3	Diagram of Apparatus Used for Pulling Crystals by the Czochralski Technique Under B ₂ O ₃ Glass	9
4	Energy Levels at $k = 0$ in Semi-insulating GaAs, According to a Modified Blanc-Weisberg Model ⁹ and Experiment ⁸	14
5	The Carrier Concentration in Undoped GaSb at 300°K and 77°K as a Function of the Stoichiometry of the Melt	21
6	Experimental Arrangement for the Calorimetric Measurement of Optical Absorption Coefficients	26
7	The Absorption Coefficient in High-Resistivity GaAs as a Function of the Resistivity	30
8	The Absorption Coefficient of Cr-doped GaAs at 10.6 Microns and 300°K as a Function of the Chromium Concentration in the Initial Melt	31
9	Method Used for Casting Large-Diameter Window Blanks	34
10	Cross-sections of 3-inch Diameter Cast Boule of GaAs (a) Rapidly Frozen Portion Near Top; (b) Large Grain Portion Near Bottom	36

1. INTRODUCTION

With the recent development of carbon dioxide laser, emitting at 10.6 microns, particularly those having high power outputs, the selection and fabrication of suitable window materials has become a problem. The classical window materials for this wavelength region are the halide salts, such as sodium chloride or potassium bromide. While the bulk optical absorption coefficients of this class of materials are small, their physical properties leave much to be desired. They are hygroscopic (which leads to high surface optical absorption), soft and difficult to work. At high power levels they suffer from thermal fracture. Non-oxide glasses formed from the heavy elements show much improved physical properties and can be cast in large sizes. However, their absorption coefficients and poor thermal properties lead to thermal runaway and fracture. Semiconductors have excellent physical properties and can be easily worked. Their thermal properties are usually markedly better than either of the above classes of material. Their absorption coefficients are higher than those of the halide salts, but comparable with those of the chalcogenide glasses. For a more complete discussion of the above problem the reader should consult references 1 and 2.

The criteria for selecting a suitable semiconductor material are quite easily stated, but the choice inevitably involves a compromise.

The material should have very few free carriers at the temperature at which it is to be used--we are assuming here that normal ambient conditions of $300 \pm 30^\circ\text{K}$ apply (other materials become suitable at lower temperatures). In order that thermal generation of carriers be small, the fundamental (or lowest) energy band gap should be greater than approximately 0.7 eV. On the other hand the band gap should not be too high for the more covalent semiconductors, since the lighter atoms involved will raise the phonon frequencies to the point where they cause appreciable absorption at 10.6 microns. For some types of operation a high thermal conductivity is required, and this property gets poorer as the ionicity of the material increases. The physical properties required will depend on the application, but usually the material has to be inert in a variety of atmospheres at normal temperatures and hard so that it may be worked easily.

Of the group IV materials, silicon can be made sufficiently pure that the free-carrier absorption is negligible, but the phonon bands tail is too large for laser use. Germanium has been widely used, but has to be cooled due to thermal runaway problems caused by its low energy band gap. Edge cooling of germanium windows leads to problems of thermal gradients and hence variations in refractive index and optical flatness. It also adds considerably to the weight and mechanical complexity of the laser.

Examining the III-V materials the aluminum compounds and the phosphides

have phonon summation bands at too short a wavelength; then only GaSb and GaAs satisfy the band gap criterion. These two have been selected for this study and will be discussed in detail later.

The II-VI materials suffer from poorer thermal conductivity and increased ionicity but candidates such as CdTe, ZnSe or ZnTe may well prove excellent for some applications. Unfortunately present technology can only provide relatively small single or polycrystalline samples of sufficient purity, due mainly to the high temperatures and/or pressures required for synthesis.

The objective of this work is therefore to concentrate on GaAs and GaSb, particularly the former since it can be prepared in high resistivity form, and to examine the optical absorption process at 10.6 microns and optimize the material for CO₂ laser window use. The development of material in a size considerably larger than that presently available commercially is also being undertaken.

2. CRYSTAL GROWTH

2.1 GaAs - Sealed System Technique

The equipment used to pull GaAs consists of the sealed system shown in Figure 1. All parts exposed to the inner chamber are of fused quartz with the exception of the crucible. During these studies the crucible material used was alumina. Seed rotation and height control are achieved by magnetic coupling between the high Curie temperature metal and magnets mounted externally to the tube and heaters, after a method first proposed by Gremmelmaier.³

High purity gallium (6N+) is loaded into the crucible while high purity arsenic (6N) is sublimed into the upper part of the chamber. After flushing and evacuating the tube is backfilled to 150 torr with helium and sealed off. After installation in the crystal pulling equipment the seed is raised completely clear of the melt. The RF generator is then turned on and the melt heated by direct coupling to approximately 1,250°C. The resistance heaters which completely surround the tube are then turned on and the arsenic is driven down until the melt is stoichiometric. The amount of arsenic loaded is sufficient to give this condition and leave an excess arsenic pressure of approximately one atmosphere.

The freezing point of the GaAs melt is then established visually. After raising the temperature slightly the seed is lowered until it touches

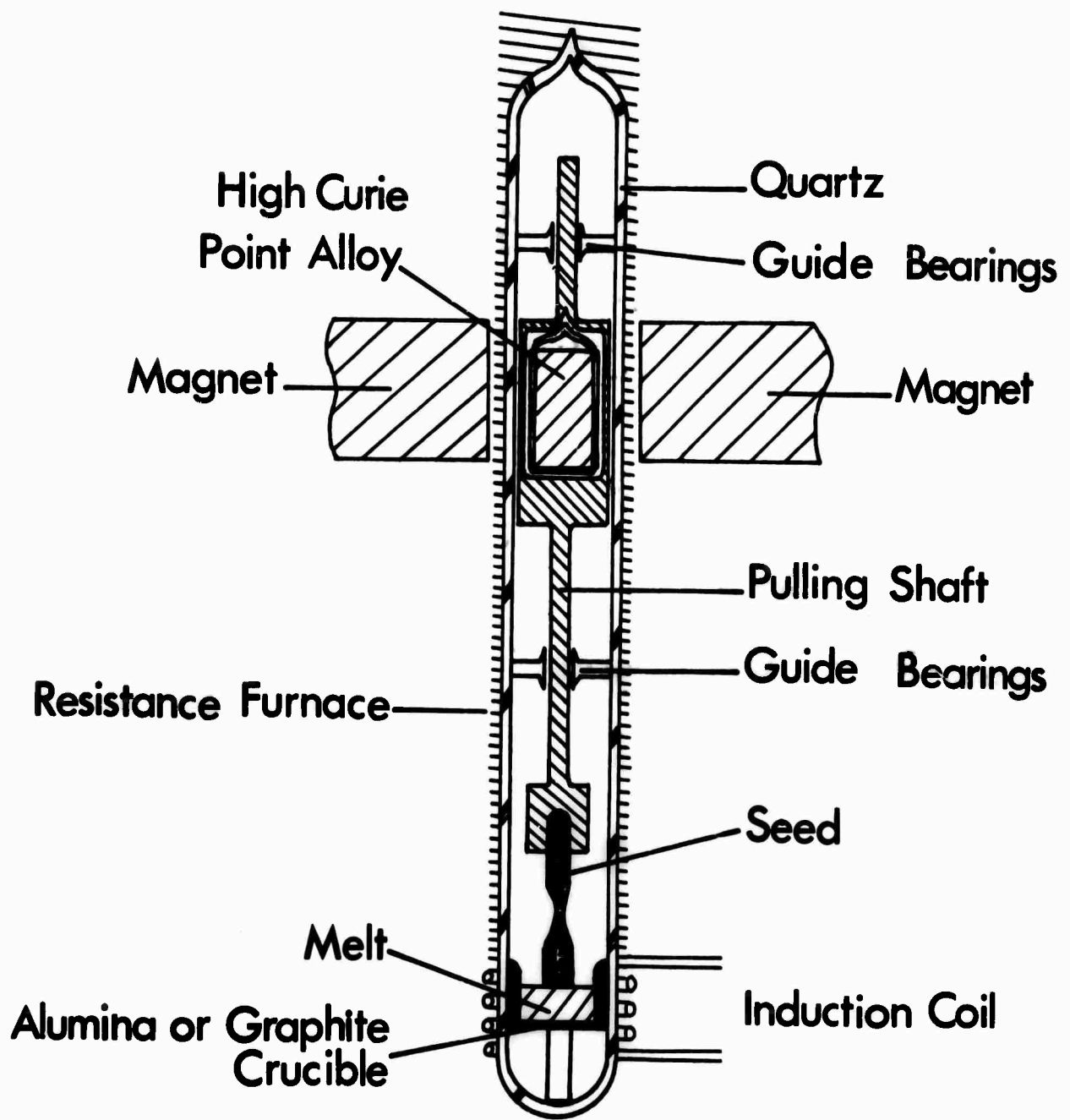


Figure 1. Diagram of Apparatus Used for Pulling Crystals by the Sealed Czochralski Technique

2. CRYSTAL GROWTH

2.1 GaAs - Sealed System Technique

The equipment used to pull GaAs consists of the sealed system shown in Figure 1. All parts exposed to the inner chamber are of fused quartz with the exception of the crucible. During these studies the crucible material used was alumina. Seed rotation and height control are achieved by magnetic coupling between the high Curie temperature metal and magnets mounted externally to the tube and heaters, after a method first proposed by Gremmelmaier.³

High purity gallium (6N+) is loaded into the crucible while high purity arsenic (6N) is sublimed into the upper part of the chamber. After flushing and evacuating the tube is backfilled to 150 torr with helium and sealed off. After installation in the crystal pulling equipment the seed is raised completely clear of the melt. The RF generator is then turned on and the melt heated by direct coupling to approximately 1,250°C. The resistance heaters which completely surround the tube are then turned on and the arsenic is driven down until the melt is stoichiometric. The amount of arsenic loaded is sufficient to give this condition and leave an excess arsenic pressure of approximately one atmosphere.

The freezing point of the GaAs melt is then established visually. After raising the temperature slightly the seed is lowered until it touches

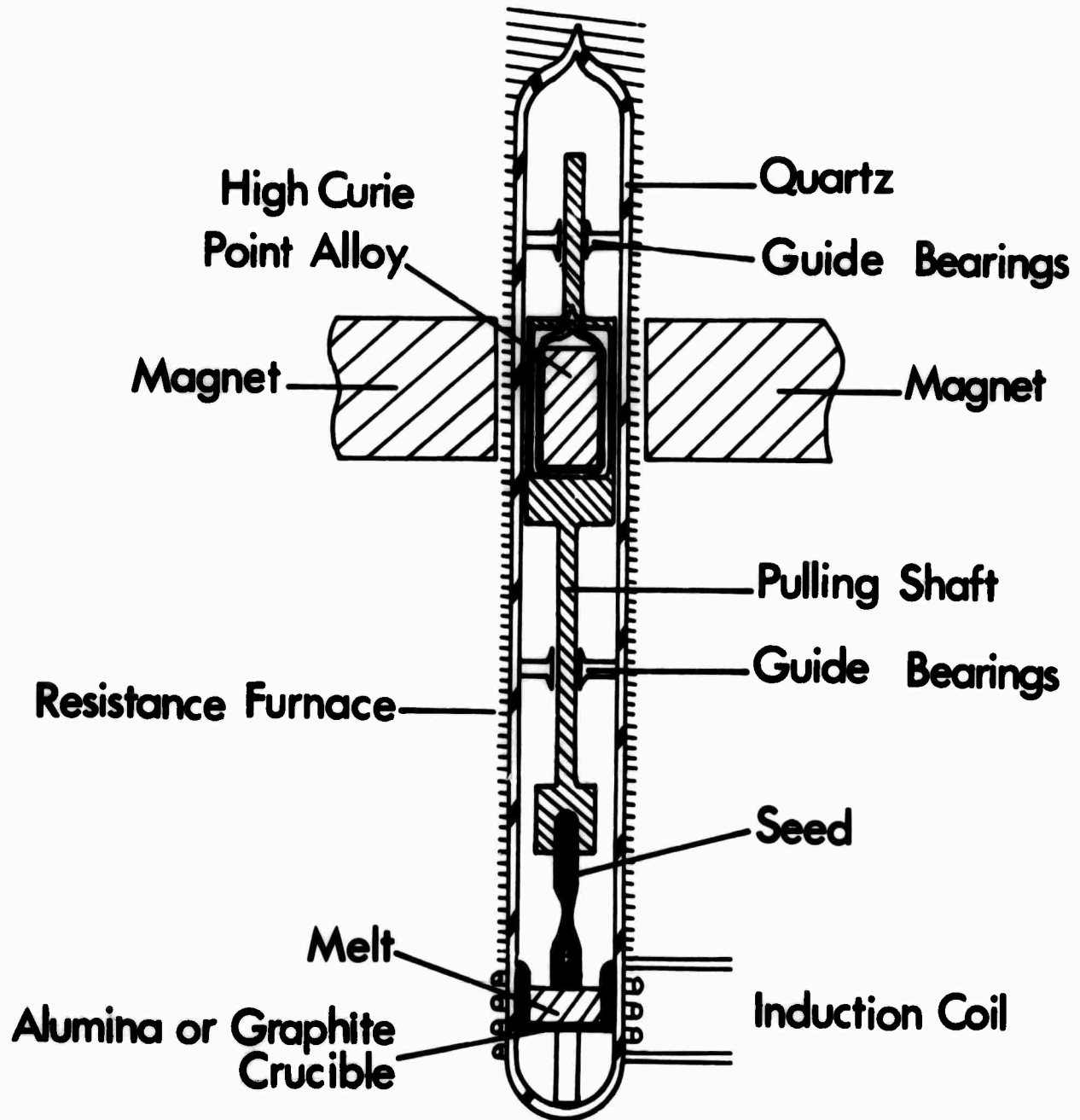


Figure 1. Diagram of Apparatus Used for Pulling Crystals by the Sealed Czochralski Technique

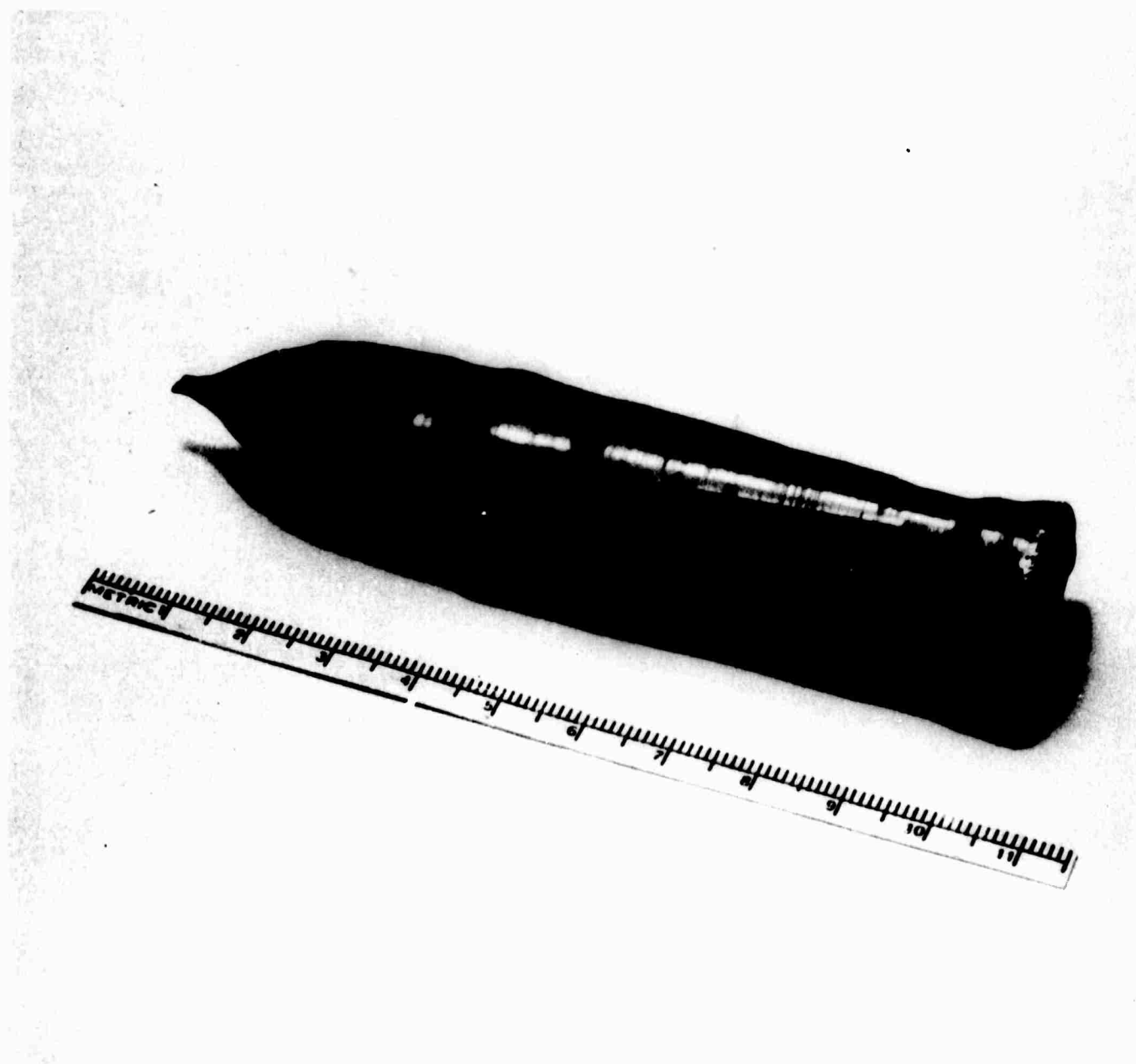


Figure 2. A Typical $\{111\}$ Cr-doped GaAs
Single Crystal Ingot

the melt. Growth then commences with diameter control being achieved by temperature control of the melt. For this study a growth rate $\sim 2 \text{ cm hour}^{-1}$ was employed, while the rotation rate was usually 10 rev min^{-1} . Should the initial growth contain grain boundaries or the neck not be of the desired shape or length the seed is lowered back into the melt far enough to remove the anomaly. The operator watches the growth operation through a small window at the bottom of the resistance heater, which is not shown in Figure 1 for the sake of clarity. A gas torch keeps the window warm enough to prevent arsenic condensation or non-uniform temperature gradients.

Figure 2 shows a typical Cr-doped GaAs ingot of the type used in this study. The long axis of the ingot is oriented $[111]$, with three flats being visible near the neck since a seed with a (111) arsenic face was used. The sizes of the ingots grown during the course of this work ranged from 2 - 3 cm in diameter with a length of 9 - 12 cm. The measurements made on these ingots are discussed in Sections 3 and 4.

2.2 GaAs - Liquid Encapsulation Techniques

In order to evaluate GaAs as completely as possible, ingots were pulled by another technique, namely liquid encapsulation. The apparatus used is shown in Figure 3. Here the seed rotation and height control is done by mechanical coupling. There is also provision for crucible rotation and height control, but these features were not utilized during the

course of this work since an adequate temperature gradient could be maintained during ingot growth. The melt is contained in a crucible and encapsulated in a liquid glass. By maintaining an inert gas pressure in excess of the arsenic pressure at the melting point of GaAs on the liquid glass stoichiometry can be maintained. This technique was first used by Metz et al⁴ to prepare PbSe and PbTe and was later applied to other materials.^{5,6}

Pieces of GaAs are loaded into the quartz crucible and a slug of the encapsulant placed on top of the GaAs. The encapsulant used here was boric oxide, which was prepared by heating boric acid in a platinum crucible for several days at 1,000°C. After pumping and flushing the chamber the boric oxide is melted and baked out under vacuum for a day, in order to remove as much water as possible. If this is not done it turns opaque during crystal growth. The heater is then removed and the RF coil is positioned correctly. The RF power is then turned on and coupled to the graphite susceptor which heats the melt. At the same time the chamber is pressurized to about two atmospheres with high-purity helium or nitrogen. When the melting point of GaAs has been exceeded by 20 or 30°C, the melt is allowed to homogenize for an hour or so before growth is commenced in the usual manner.

Ingots grown in this system are typically 3 cm in diameter and 6 to

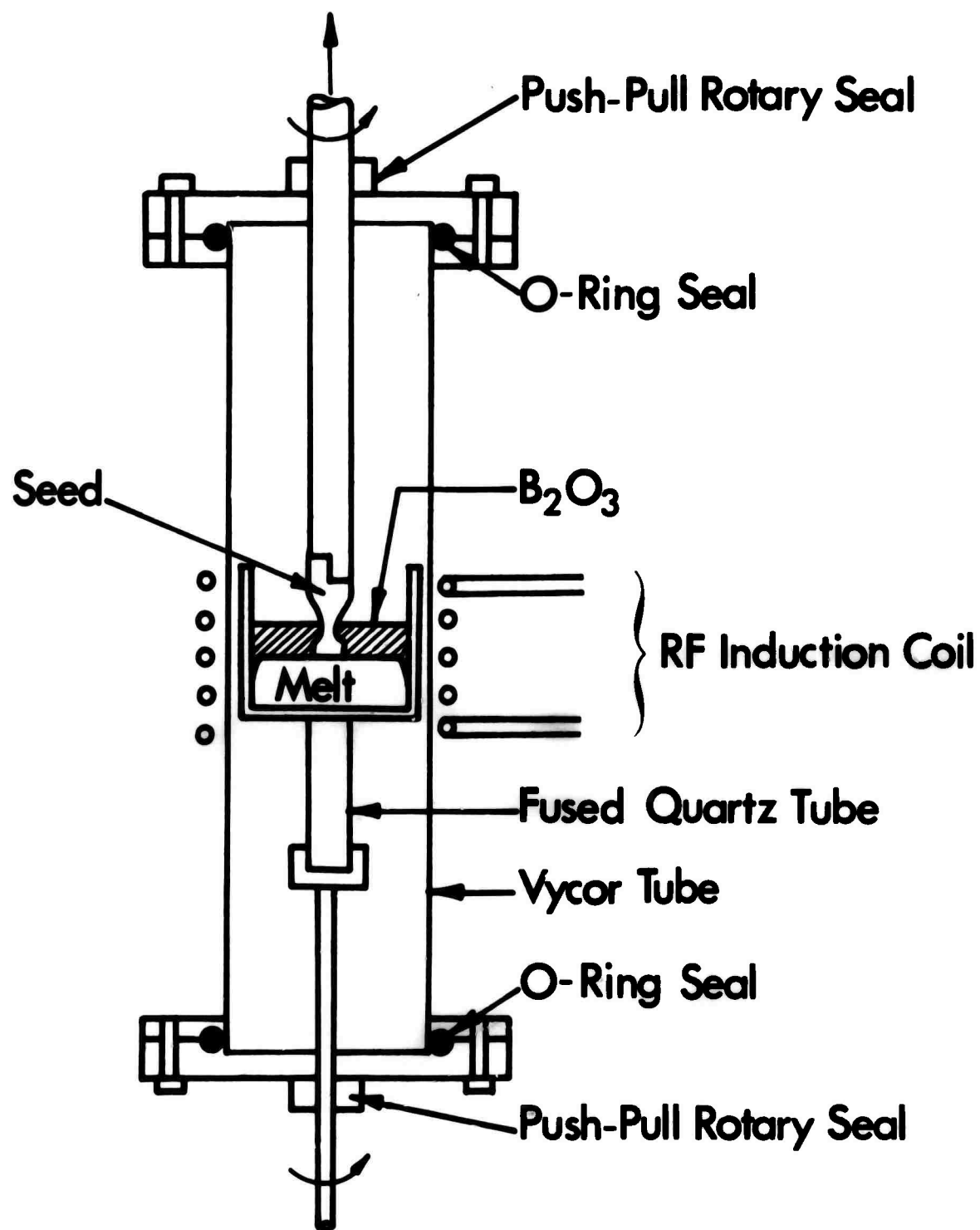


Figure 3. Diagram of Apparatus Used for Pulling Crystals by the Czochralski Technique Under B₂O₃ Glass

12 cm long. Growth parameters for GaAs were kept at a 1.5 cm hour^{-1} growth rate and a 6 rev min^{-1} rotation speed. As for the sealed system technique [111] oriented seeds were used.

2.3 GaSb - Growth Techniques

The GaSb was prepared in a crystal pulling apparatus similar to that shown in Figure 3. Because of the lower melting point of GaSb resistance heating is employed, replacing the RF coil and graphite susceptor shown in the diagram. Crystal growth was performed both with and without the boric oxide encapsulant. In the former case a casting was prepared by melting under vacuum the desired amounts (see Section 3) of high purity gallium* and antimony** together in a quartz container, homogenizing and quenching in water. This charge was then transferred to the growth apparatus, the boric oxide added and growth commenced in a manner similar to that described in Section 2.2. This method has the disadvantage that volatile impurities cannot volatilize, forming a scum on the melt surface and inhibiting single crystal growth.

The best ingots, particularly from non-stoichiometric (antimony-rich) melts, were obtained without using an encapsulant. Here the antimony was melted under hydrogen and thus purified somewhat. It was then loaded with

* Alusuisse, 6N+.

** United Mineral and Chemical Corp., 6N.

the gallium, and by quickly raising the temperature the oxides on the gallium were volatilized. High-purity hydrogen at a pressure of two atmospheres sufficed to keep the melt reasonably clean, while antimony sublimation was not too serious even for the non-stoichiometric melts.

Growth conditions varied, but for the extreme case of a 70:30 (Sb:Ga) melt a minimum growth rate of 2 mm hour^{-1} was used. A rotation speed of approximately 6 rev min^{-1} was used in all cases. Ingot sizes ranged from 1 cm diameter by 2 cm long from the non-stoichiometric melts up to a 3 cm diameter by 10 cm long from stoichiometric melts. Once again (111)B oriented seeds were used.

3. PHYSICAL AND ELECTRICAL PROPERTIES

3.1 Semi-insulating GaAs

Relatively uncompensated GaAs grown from stoichiometric melts typically contains one to two ppm of electrically-active impurities, corresponding to an n-type carrier concentration in the low 10^{16} cm^{-3} region. However, certain dopants have been shown to be capable of reducing this carrier concentration by orders of magnitude, yielding room temperature resistivities from 10^3 to 10^8 ohm-cm, the latter being close to the calculated intrinsic value for GaAs. The dopants which have commonly been used are the transition metals such as iron, cobalt and nickel and other elements including chromium, oxygen, copper and zinc. A brief bibliography of this work is given in References 7 and 8. Most of these elements apparently give one or more deep levels,⁸ with zinc being the exception. It gives a shallow acceptor and the amount needed to compensate the shallow donors is very critical; this mechanism is assisted by the small amounts of chromium, iron, etc., which are usually present in GaAs.

The accepted mechanism for the semi-insulating state is based on a model originally proposed by Blanc and Weisberg.⁹ They suggested shallow donor and acceptor levels close to the conduction and valence band edges respectively and a deep donor close to the center of the energy gap. If this deep donor is replaced by a deep acceptor the observation of both n-

and p-type semi-insulating material can be explained without the need for close compensation. Figure 4 shows the proposed energy band diagram for GaAs at $k = 0$. With this model the number of deep acceptor impurities only has to exceed $(N_D - N_A)$ to give essentially intrinsic behavior. This statement will be discussed later in this section.

3.2 Physical Properties of GaAs

The GaAs ingots grown by both the sealed system technique and the liquid encapsulation technique were evaluated for crystallinity and dislocation density. Evaluation slices were cut from just below the crown and the bottom of the single crystal portion of the ingot. These were lapped, chemically polished ($\text{HF}:\text{HNO}_3:\text{H}_2\text{O}$, 1:3:4; 5 minutes) and etched to reveal dislocations ($\text{HNO}_3:\text{H}_2\text{O}$, 1:2, 5 minutes). The counting of dislocations was done in five different areas and any tendency toward lineage or grain boundaries noted. The crystals grown by the sealed system technique typically contained $\sim 10^4 \text{ cm}^{-2}$ at the top and $\sim 10^5 \text{ cm}^{-2}$ at the bottom. The liquid encapsulation crystals were usually lower by half an order of magnitude. Only material without noticeable patterns of dislocations was used for the optical measurements. In all, about twenty ingots of GaAs yielded material of sufficiently high quality for the electrical and optical measurements.

3.3 Impurities in GaAs

The evaluation slices described above were used to provide Hall bars

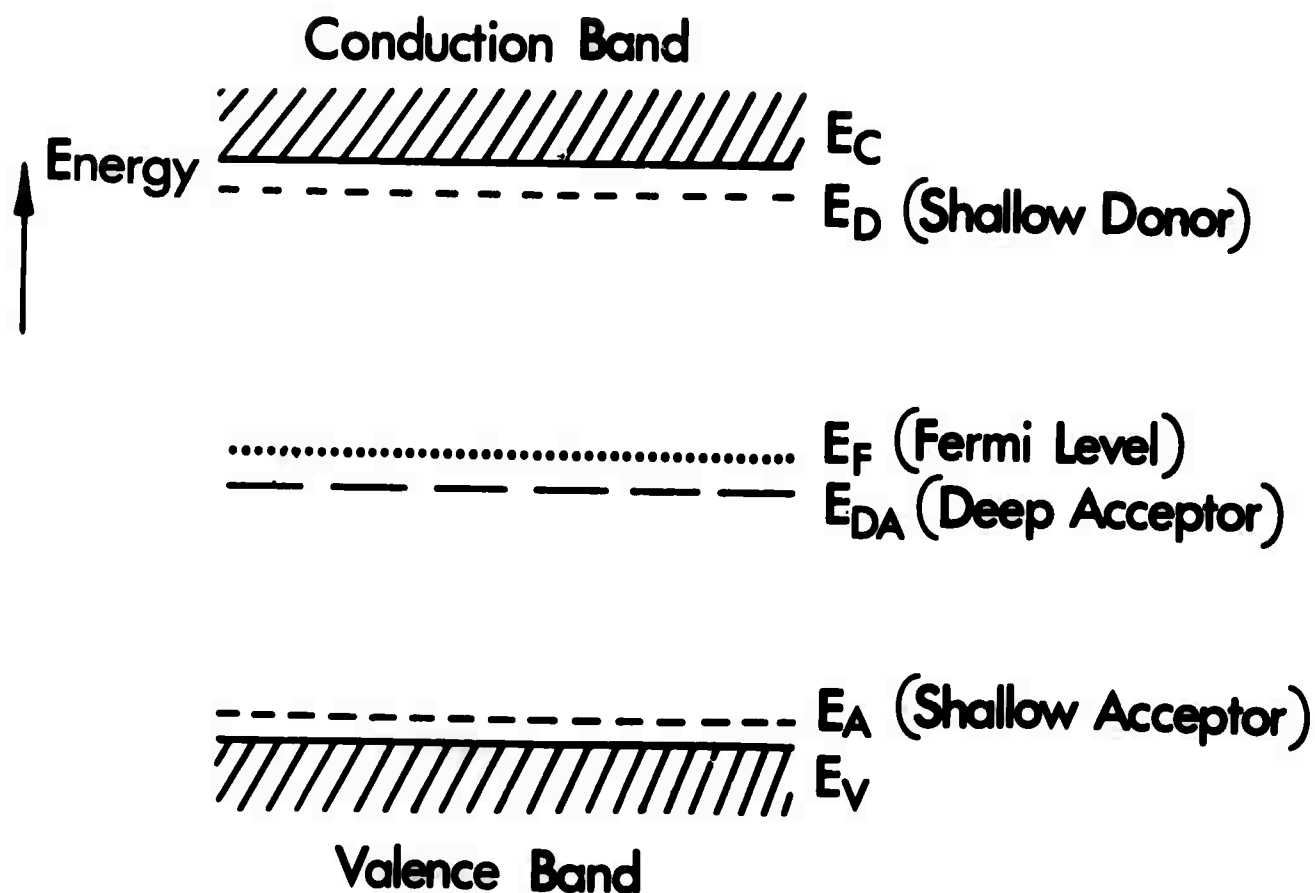


Figure 4. Energy Levels at $k=0$ in Semi-insulating GaAs, According to a Modified Blanc-Weisberg Model⁹ and Experiment⁸

(see next sub-section) and small bars for spark source mass spectrometric analysis. The latter were usually lapped, degreased and etched (in HNO_3 : $\text{HF}:\text{H}_2\text{O}$, 1:1:1) sufficiently to remove an appreciable amount of material. Clean procedures were followed until the loading of the mass spectrometer was complete. The instrument used (a modified CEC X21-110) has ion pumping with adequate cold-trapping. All elements were examined, and the following is a summary of the results.

Sealed System GaAs (Cr-doped):

Cu	< 0.05 ppma
Li, B, P	< 0.1 ppma
N, Fe, Ni, Mn	< 0.5 ppma
Si	~ 0.5 ppma
S	~ 1 ppma
Ca	0.1 - 1 ppma
F	0.1 - 5 ppma
K	0.5 - 5 ppma
C	1 - 3 ppma
O	1 - 5 ppma
Al	1 - 10 ppma
Cr	1 - 10 ppma (usually 1 - 2 ppma).

All other elements have a detection limit of 0.3 ppma or less and were not detected. Fe, Ni and Mn were usually below their detection limit ~ 0.2 ppma, but traces were seen in the more heavily Cr-doped samples. Some of the N, O, F and C comes from the cleaning and handling procedures or residuals in the instrument, while the aluminum is traceable to the use of alumina crucibles. Undoped ingots grown with similar starting

materials usually have similar impurity levels except for the iron and nickel which usually do not appear at all.

Liquid Encapsulation GaAs (Cr-doped):

Similar to above except for

B	~ 0.5 ppma
Al	< 1 ppma
Si	~ 0.3 ppma
S	~ 0.5 ppma
P	< 0.3 ppma.

Sealed System GaAs (Fe-, Ni-doped)

Similar to Cr-doped grown in the same system, with

Cr	< 0.2 ppma
Fe	1 - 5 ppma
Ni	1 - 2 ppma (with Ni doped showing ~ 0.5 ppma of Mn).

The above show some variations but the dopant levels and electrically active impurities seem to be quite well defined. On the whole the liquid encapsulated Cr-doped GaAs is purer than the sealed system material. Electrical measurements on undoped material bear this out, with the encapsulated material being n-type with mid- 10^{15} carriers cm^{-3} and the sealed system material n-type with low 10^{16} carriers cm^{-3} (see next Section).

An attempt was made to see if the chromium was segregating on a microscopic scale, as has been suggested. Using a Cameca/Bell & Howell Direct Imaging Mass Analyzer, Model 27-201 several typical Cr-doped GaAs

specimens were examined for the distribution of chromium and other major impurities (S, Si, Al and transition metals). With an approximate spatial resolution of one micron no clumps or vacant spots could be detected in any of the samples (which contained between 1 and 8 ppma of chromium). The amount of each impurity present (when measured rather qualitatively) agreed well with the mass spectrometric results.

The distribution coefficients of Cr, Fe and Ni in GaAs for a {111} growth direction and pull speed $\sim 2 \text{ cm hr}^{-1}$ were calculated from the mass spectrometric data and a knowledge of the amounts of dopant added to the melt. Using the formula¹⁰

$$C = kC_0 (1 - g)^{k-1}$$

where C_0 and C are the impurity concentrations in the initial melt and after a fraction g of the melt has been pulled respectively, and k is the distribution coefficient defined as

$$k = \frac{\text{ppma of dopant in first-to-freeze portion of ingot}}{\text{ppma of dopant in total initial melt}}$$

we find that for small $k (< 10^{-2})$ we may write

$$\frac{C_1}{C_2} = \frac{1 - g_2}{1 - g_1}.$$

In this manner the concentrations at the top and bottom of the ingot were

corrected to the first-to-freeze point. Plotted on a log/log plot against the amount of dopant contained in the starting melts straight lines of slope = 1 were obtained for chromium (over 0.6 - 8 ppma) and iron (over 1 - 4 ppma) with some indication of a levelling-off at lower impurity levels. Only two points were obtained for nickel (at 1 ppma), but these agreed well with each other. The mean results obtained are

$$k_0 (\text{Cr}) = 6.0 \times 10^{-4}$$

$$k_0 (\text{Fe}) = 6.4 \times 10^{-4}$$

$$k_0 (\text{Ni}) = 4 \times 10^{-5}$$

These results confirm earlier work performed here by Willardson and Allred.¹¹ This reference also surveys the literature critically.

3.4 Electrical Properties of Semi-insulating GaAs

Resistivity measurements were made on ultrasonically cut bridge-shaped samples. After thorough cleaning the samples were contacted with indium or tin in a reducing atmosphere at 450°C for one to two minutes. After soldering wires to the contacts the sample was degreased and placed in a light-proof holder. The measurement was performed with a teraohmmeter. Although the accuracy of this method is not very good, it is adequate since a resistivity range from 10^3 to 10^8 ohm-cm was found. All electrical measurements were done at room temperature.

Most of the Cr-doped ingots exhibited resistivities between 10^6 and 10^8 ohm-cm, with the latter corresponding to the heavier doped material. At the lower doping levels the resistivity would revert very quickly to normal "undoped" levels if the amount of chromium were insufficient to overcome the net donor density. Thus usually approximately one ppma of chromium was required in order to yield high-resistivity material. The Fe-doped GaAs behaved in a similar manner except the resistivity range varied from 10^4 to 10^6 ohm-cm. Again, approximately one ppma of iron was sufficient to give high-resistivity material. The one Ni-doped ingot grown during this period had a resistivity of 3,700 ohm-cm at the top and 12 ohm-cm at the bottom. This is because the net donor density increased along the ingot to a level that the nickel could not compensate.

No Hall measurements have been made on these materials to date. Other workers have reported quite widely varying results, with carrier concentrations between 10^7 and 10^{11} cm^{-3} and mobilities of $10 - 1,000$ $\text{cm}^2\text{V}^{-1}\text{sec}^{-1}$ (see for example References 7, 12 and 13). One clue to the behavior is the rapid change in Hall coefficient and mobility with temperature¹³ around 290°K.

3.5 Properties of GaSb

The GaSb ingots, particularly those grown from non-stoichiometric melts, were quite small and hence only one evaluation slice was taken. This provided a Hall bar and pieces for the mass spectrometric analysis. Dislo-

cation densities were not measured, especially since some of the ingots were twinned or polycrystalline. The mass spectrometric results revealed little difference between the liquid encapsulated and normal material. Due to the difficulties with the former, most of the ingots were grown without boric oxide. The presence of Mg, P, S, Cr, Fe and Zn in ppma quantities or less was observed, while Al, Si, K, Ca and Na were erratic but present up to 10 ppma at times. Oxygen was usually seen at levels on the order of 100 ppma. The Cr- and Te-doped ingots contained the expected amounts of dopant.

The electrical properties of GaSb were investigated by taking Hall measurements on a bridge-shaped sample at 300°K and 77°K in a magnetic field of 20 Kgauss. The contacts to the bar were made with tin spheres alloyed quickly at 450°C in a reducing atmosphere. All the materials were p-type and the single carrier Hall formula was used assuming a scattering coefficient $r = 1$. The variation of carrier concentration with the stoichiometry of the melt from this and previous studies is shown in Figure 5. Also shown are the results of Reid et al¹⁴ and good agreement was obtained. The mobilities we observed ranged up to $5,500 \text{ cm}^2 \text{ V}^{-1} \text{ sec}^{-1}$ at 77°K for an ingot pulled from a 30:70 GaSb melt.

The dominant carriers in GaSb are caused by vacancies which depend on the stoichiometry of the melt, as is discussed in References 14 and 15 for

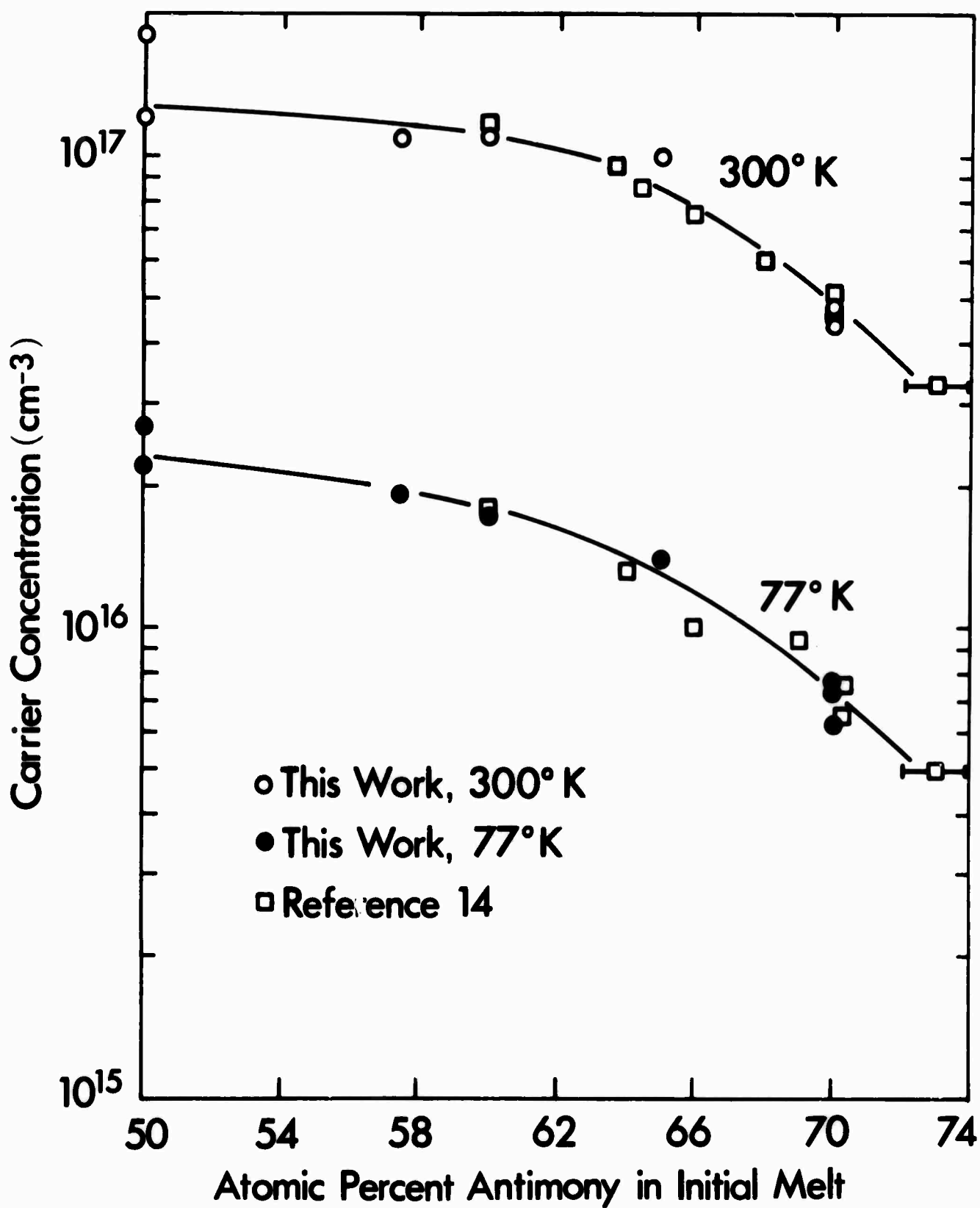


Figure 5. The Carrier Concentration in Undoped GaSb at 300°K and 77°K as a Function of the Stoichiometry of the Melt

example. Thus GaSb may be easily doped n-type with Se, Te, etc., so long as the number of n-type carriers is sufficient to overcome the number of p-type carriers due to vacancies. The addition of chromium to GaSb grown from non-stoichiometric melts did not significantly change carrier concentrations or mobilities (these averaged $\rho = 5 \times 10^{16}$ and $7 \times 10^{15} \text{ cm}^{-3}$ at 300°K and 77°K respectively; $\mu = 900$ and $5,000 \text{ cm}^2 \text{ V}^{-1} \text{ sec}^{-1}$ at 300°K and 77°K respectively). The chromium did go into solution and appeared in the ingots in the four ppma range as verified by the mass spectrometer. Attempts to dope lightly with tellurium to give $n < 10^{17} \text{ cm}^{-3}$ and chromium to give deep levels have been unsuccessful to date, partly due to an inadequate knowledge of the distribution coefficient for tellurium at these impurity levels. Also other dopants have not yet been tried. It is anticipated that one of the transition metals should give a level near the center of the energy gap which would result in high-resistivity material suitable for window use at room temperature.

4. OPTICAL PROPERTIES

4.1 Optical Properties of GaAs

The optical properties of GaAs have been well documented at energies above, close to and below the fundamental gap (see chapters 2, 4, 5, 6 and 9 of Reference 16). In the region of interest, close to 10.6 microns, the properties have only been examined for samples having free carrier absorption. Thus Cochran et al¹⁷ show an absorption coefficient that is essentially zero on their scale up to 12 microns for a high resistivity sample of GaAs. However with conventional techniques and thin samples absorption coefficients in the 0.01 cm^{-1} range are very difficult to measure absolutely. In the next sub-section we discuss this problem further.

Several reasons have been advanced attempting to explain the small ($\sim 0.01 \text{ cm}^{-1}$) residual absorption coefficient at 10.6 microns in GaAs in which free-carrier absorption is negligible. The presence of multiphonon bands in the general region has been shown^{17,18} but their magnitude at 10.6 microns is probably small since the three-phonon bands occur at longer wavelengths and the four-phonon bands at shorter wavelengths. Klein and Rudko¹⁹ use a homological argument to suggest that a fourth-order electric moment could give an absorption approximately 0.03 cm^{-1} in GaAs at 10.6 microns. Nicolai and Gottlieb²⁰ postulate a coupled mode involving the electronic polarizability of the material based on measurements on a variety of mater-

ials. The resolution of these arguments depends on accurate measurements of the optical absorption coefficient in pure materials over a spectral range, rather than at one wavelength for a specific purpose as is being done here.

The effects of free carriers may be readily calculated since absorption data on doped GaAs are well documented. Using the results summarized by Fan (Chapter 9 of Reference 16), the absorption coefficient α is given by

$$\alpha = \sigma_n \cdot n$$

where σ_n is proportional to the wavelength raised to a power k . For GaAs at 10.6 microns and 300°K we obtain an $\alpha = 10^{-3} \text{ cm}^{-1}$ for $n = 1.3 \times 10^{13} \text{ cm}^{-3}$. Assuming the mobility of high resistivity material in this carrier concentration range is approximately $100 \text{ cm}^2 \text{ V}^{-1} \text{ sec}^{-1}$ this is equivalent of a resistivity of approximately $6 \times 10^3 \text{ ohm-cm}$.

Therefore, if the resistivity of GaAs exceeds approximately 10^4 ohm-cm the additional optical absorption due to free carriers will be negligible compared with the fundamental absorption coefficient (which is approximately 0.01 cm^{-1}). In Section 4.3 curves are presented showing the variation of α (free carriers) with resistivity.

4.2 Measurement of Optical Absorption Coefficient

The technique chosen here to measure the optical absorption coefficient of semiconductors at 10.6 microns is a calorimetric one. This method lends itself to the measurement of small absorption coefficients (in the 0.01 to 0.1 cm^{-1} range) with reasonable precision and is quick to perform both from sample preparation and actual measurement points of view.²⁰ Another advantage is the fact that a CO_2 laser is used for the measurement at precisely the same wavelength that the material will be used for windows.

We have followed the general method of Weil,²¹ who discusses the various calorimetric techniques used previously. The apparatus is shown schematically in Figure 6. A Sylvania Model 941 frequency stabilized CO_2 laser gives an approximately parallel 5mm diameter beam of 10.6 micron radiation at a power of 5W. The light passes through the sample and is detected and measured by a Coherent Radiation Model 201 power meter. The sample is mounted in a double chamber on top of a brass post.²⁰ No windows are used so that the formula (#21) of Reference 21 may be directly applied.

The samples used were cut perpendicular to the growth direction of the ingot so their faces were approximately {111} planes. The sides were lapped and mechanically polished, finished thicknesses falling in the range of 3 to 7mm. A ground flat on the edge of the disc was used to mount the sample on a small platform at the top of the brass post. A differential thermo-

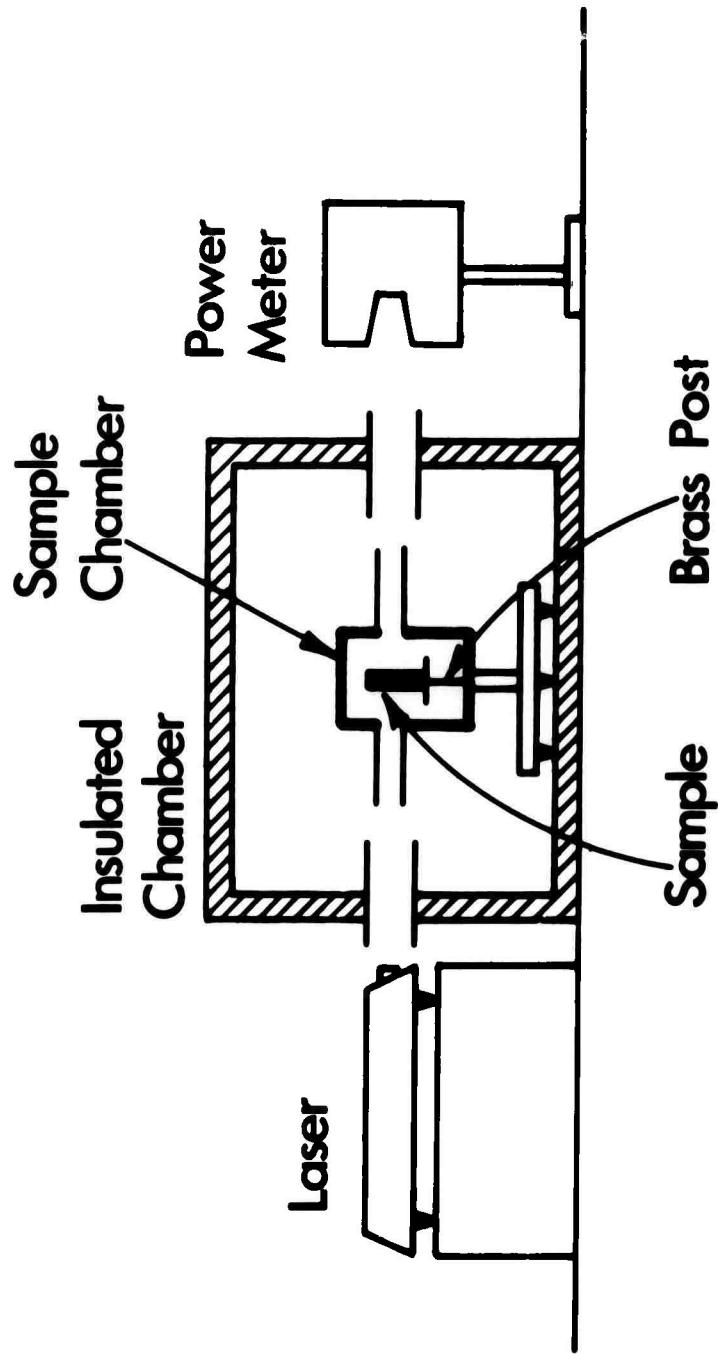


Figure 6. Experimental Arrangement for the Calorimetric Measurement of Optical Absorption Coefficients

couple is used to monitor the temperature difference between the top (sample) and the bottom (chamber) of the post.

After allowing the laser to warm up and stabilize the beam is allowed to fall on the sample. The temperature difference along the post is monitored at frequent intervals until it stabilizes. At that time the reading is noted, the beam blocked and the power to two resistors mounted on the platform turned on. This power is adjusted until the temperature difference is stable and equal to that caused by the laser. The knowledge of this power (P_s), the power transmitted by the sample (P_T) and the length of the specimen is sufficient to calculate the optical absorption coefficient α of the material using the formula²¹

$$\alpha = \left(\frac{P_s}{l P_T} \right) \left(\frac{2n}{n^2 + 1} \right)$$

For GaAs we have taken $n = 3.30$, although values reported in the literature range from 3.1 to 3.5. The absolute error introduced by this assumption can be no greater than $\pm 5\%$. Other errors due to different radiation losses from sample heating and resistor heating, power measurement and so on could run up to $\pm 30\%$. The relative accuracy for our equipment bearing in mind the similar sample sizes is probably $\pm 20\%$ or better. If the sample is wedge-shaped, poorly aligned or in poor thermal contact with the platform a higher value of α will generally result.

It should be pointed out that the calorimetric technique measures only absorption and not scattering, unlike the more classical methods. This difference has to be taken into account in some window applications.

4.3 Results for GaAs

Approximately 25 samples of GaAs prepared here and elsewhere have been measured during this reporting period. The values of α for GaAs at room temperature are shown in the Table, together with the resistivities and dopants. Also included are some results on Monsanto Fe-doped material, A. D. Little Cr-doped material and Tyco Laboratories undoped material. The latter could not be measured for the reasons given in the Table.

The results show very few discernible trends. Most of the GaAs having a resistivity $> 10^4$ ohm-cm has an absorption coefficient lying between 0.01 and 0.02 cm^{-1} . The plot in Figure 7 shows the absorption coefficient as a function of resistivity for all those materials measured. Also shown are two curves giving the predicted additional absorption due to free carriers, assuming a mobility of 100 $\text{cm}^2\text{V}^{-1}\text{sec}^{-1}$ (curve I) or 10 $\text{cm}^2\text{V}^{-1}\text{sec}^{-1}$ (curve II). These curves assume the constants used in Section 4.1 apply in this resistivity region. One Ni-doped sample had a resistivity of 12 ohm-cm and an absorption coefficient of 0.22 cm^{-1} , which is in reasonable agreement with curve I.

For those ingots which yielded a top and bottom sample it was found

Material	Dopant	Resistivity ohm-cm	Absorption Coefficient % cm ⁻¹	Comments
Bell & Howell, Sealed System	Cr	$\left\{ \begin{array}{l} 5 \times 10^3 \\ \text{to } 1 \times 10^4 \end{array} \right\}$	0.9 to 2.1	15 samples, average = 1.5
	Fe	$\left\{ \begin{array}{l} 3 \times 10^4 \\ \text{to } 6 \times 10^5 \end{array} \right\}$	1.5 to 1.6	3 samples
	Ni	$\left\{ \begin{array}{l} 12 \text{ to} \\ 4 \times 10^3 \end{array} \right\}$	22 to 3.4	2 samples, one with low resistivity.
Bell & Howell, Liquid Encapsulation	Cr	$\left\{ \begin{array}{l} 7 \times 10^6 \\ \text{to } 1 \times 10^8 \end{array} \right\}$	1.2 to 1.8	3 samples
A. D. Little, Liquid Encapsulation	Cr	N.M.	1.8 to 3.4	2 samples
Monsanto	Fe	N.M.	0.8 to 2.0	average = 1.4
Tyco Labs, Travelling Solvent	--	< 0.1	N.M.	Too low resistivity; samples contained Ga inclusions.

Table 1. The parameters of the GaAs studied, including the ranges of resistivity and absorption coefficient for different dopants and sources of material.

(N.M. -- not measured due to limited sample size or too low a resistivity.)

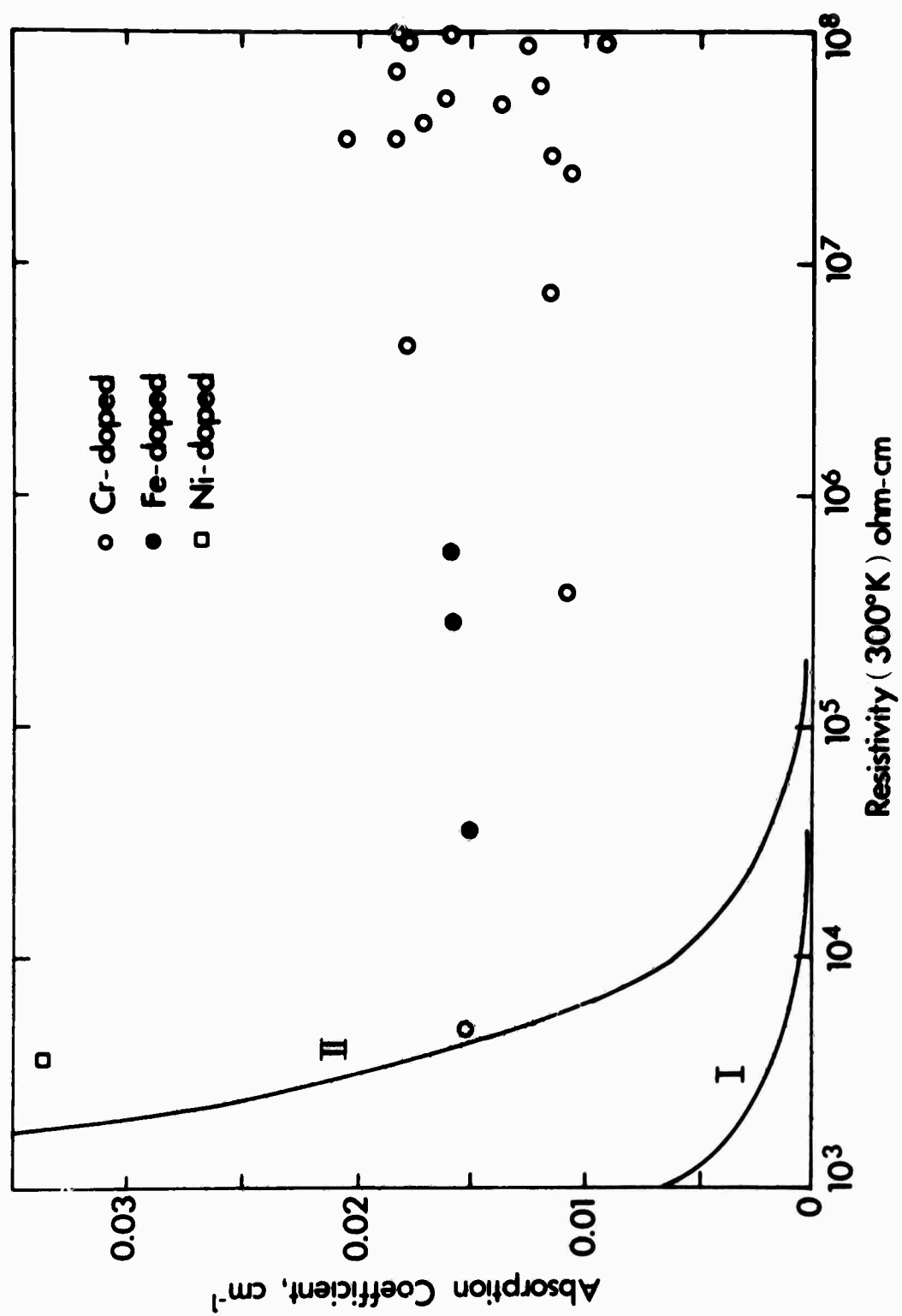


Figure 7. The Absorption Coefficient in High-Resistivity GaAs as a Function of the Resistivity

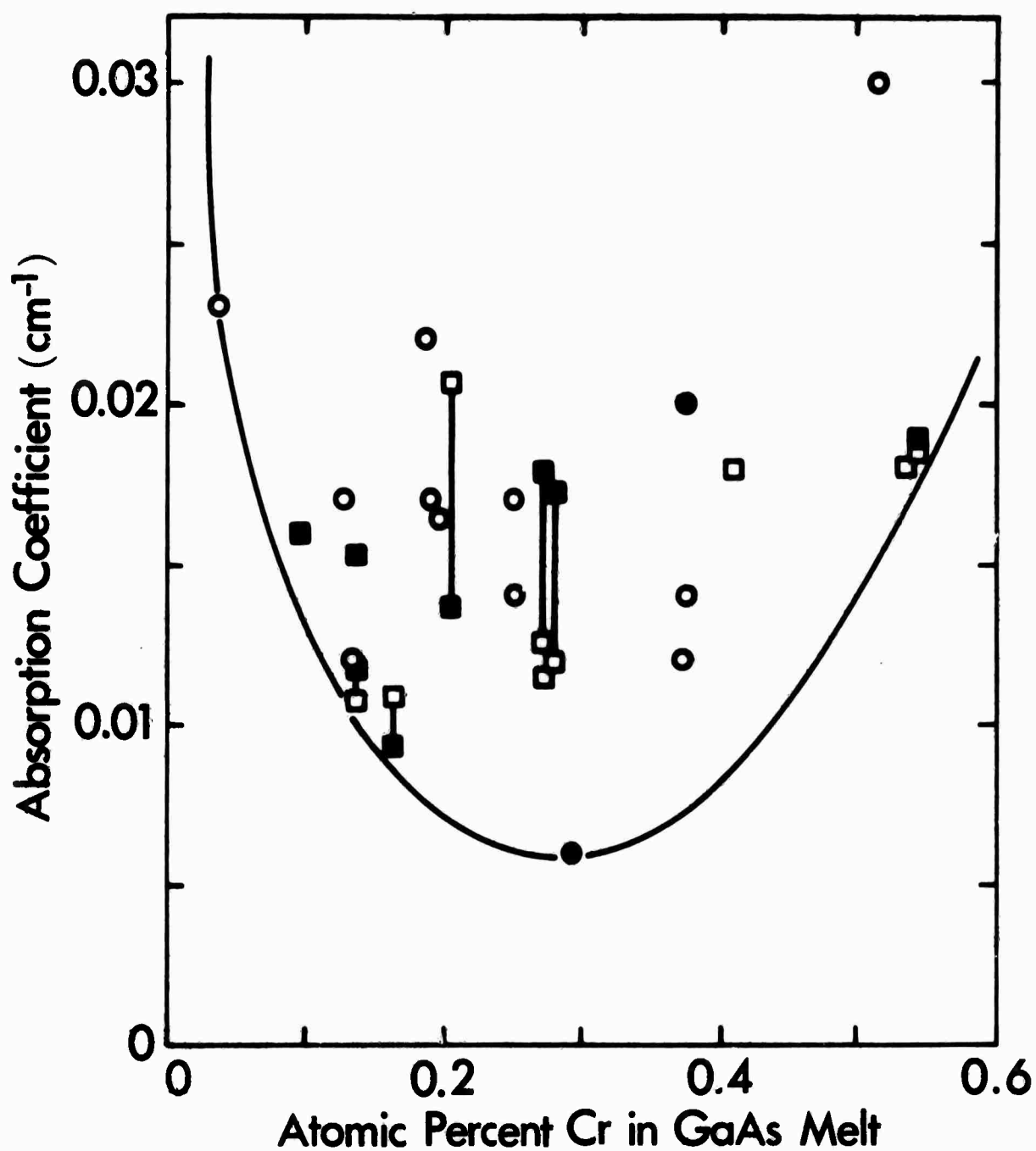


Figure 8. The Absorption Coefficient of Cr-doped GaAs at 10.6 Microns and 300°K as a Function of the Chromium Concentration in the Initial Melt

that the variation of absorption coefficient along the ingot was small, and in some cases the bottom was superior to the top. This is somewhat surprising since the impurities at the lower end are usually two to three times higher while the dislocation density is an order of magnitude greater. The latter fact is encouraging, since it indicates that stringent crystal quality is not needed for laser windows.

Figure 8 shows the absorption coefficient as a function of the amount of chromium added to the melt for Cr-doped GaAs. The points are taken from this study and two earlier studies made using our material.^{20,22} As is to be expected for low concentrations of chromium the resistivity falls and free carrier absorption can take place, while at high concentrations the excess chromium causes absorption. The broad area in between indicates an optimum Cr-concentration, but the actual location has not yet been well defined. Attempts to correlate the 10.6 micron optical absorption coefficient with the level or type of impurities present in the samples have been unsuccessful so far.

4.4 Optical Properties of GaSb

At the time of writing, no GaSb samples of sufficiently high resistivity had been prepared, and therefore none was measured optically.

5. LARGE DIAMETER GaAs

5.1 Material Preparation

In order to evaluate the feasibility of preparing GaAs boules having a diameter substantially greater than those prepared previously it was decided to start with polycrystalline material. For many window applications polycrystalline windows with large crystallites are as good as single crystal material. This criterion effectively rejects hot-pressed material whose bulk absorption coefficient is appreciably higher than the single crystal form (see e.g., Reference 2).

For the initial trials a 3" diameter was selected as a compromise, being a useful increase over the 1 - 1½" diameter pulled boules normally available and suitable for many of the higher powered CO₂ lasers. The approach taken was that of slow casting or directional freezing, since pulling a 3" diameter ingot would require a charge up to 5" in diameter.

Figure 9 shows the vessel used. The inner quartz container holds the melt of 500 to 1,000 grams of GaAs. The outer container holds the graphite susceptor in place and cushions the inner container. It also eases the pressure differential. The entire assembly is suspended from the seed rod of a crystal puller so that it may be rotated and raised or lowered smoothly. With the susceptor located centrally in the RF coil the charge is melted and allowed to homogenize. With the surface of the melt, which is usually the

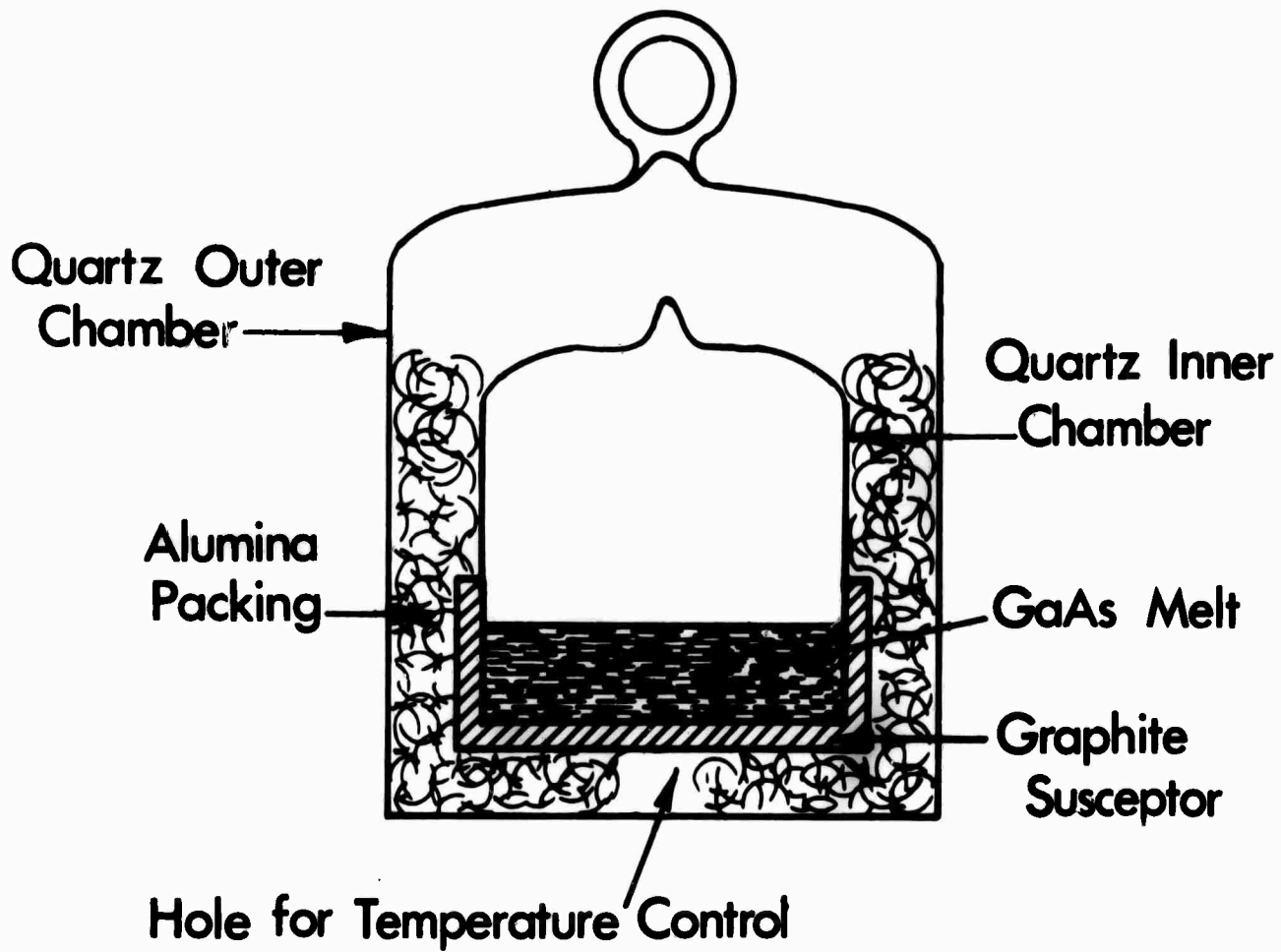


Figure 9. Method Used for Casting Large-Diameter Window Blanks

coldest part, 20°C above the freezing point the whole assembly is slowly lowered through the coil, thus causing the melt to freeze from the bottom upwards. A rotation speed of 4 rpm was used with a lowering rate (which is approximately equal to the growth rate) of 1 cm hr⁻¹.

The temperature of the melt surface has to be constantly monitored with the optical pyrometer since the coupling increases as freezing commences, and the power adjusted accordingly.

5.2 Results

Cross sections from the top and bottom of a successful casting are shown in Figure 10. The top of this piece was frozen rapidly and hence contains "blow-holes" and some gallium inclusions. However reasonably-sized grains are still visible. The first-to-freeze portion at the bottom has very nice grain structure with no evidence of inclusions, holes, etc. The largest grain has an area of well over 10 cm². This good polycrystalline growth persisted for some three-quarters of the boule depth until the rapid freezing commenced. Preliminary mass spectrometric results show a purity comparable with that of pulled material (see Section 3.3), but the optical properties have not yet been investigated. The technique seems reliable, however and further work on segregation coefficients and temperature control should yield discs having similar optical properties to the GaAs described in Section 4.

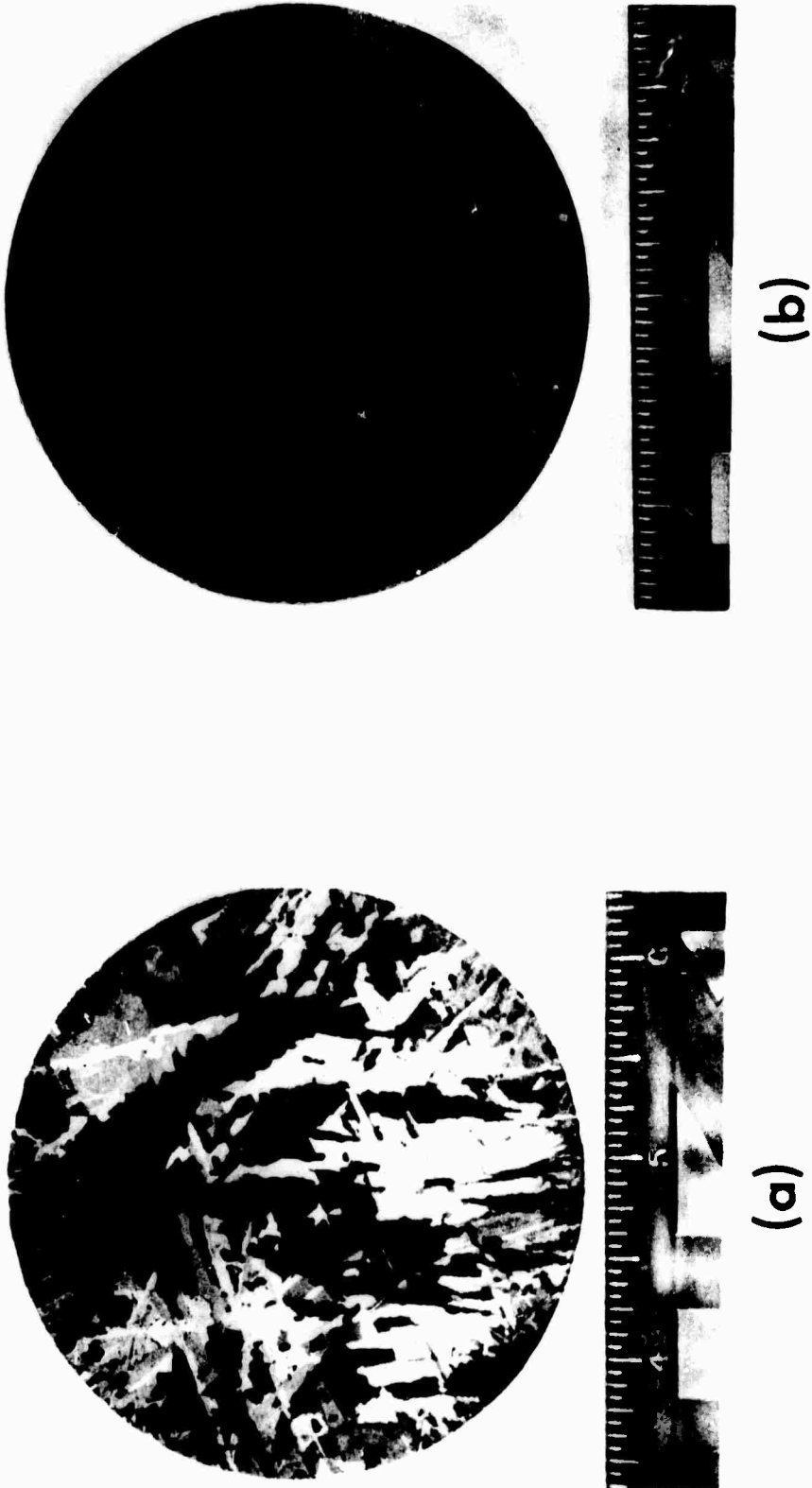


Figure 10. Cross-sections of 3-inch Diameter Cast Boule of GaAs. (a) Rapidly Frozen Portion Near Top; (b) Large Grain Portion Near Bottom

6. CONCLUSIONS AND FUTURE WORK

The variation in optical absorption coefficient at 10.6 microns for GaAs having a resistivity greater than 10^4 ohm-cm has still to be explained. We observed no significant trends for any impurity concentration or dislocation density. Still to be investigated are the effects of stoichiometry. However, GaAs with chromium doping may be reproducibly prepared with $\alpha(10.6\mu, 300^\circ\text{K}) \leq 0.015 \text{ cm}^{-1}$. The casting technique developed worked well for diameters of approximately 3" and produced large-grain material.

Further attempts should be made to produce high resistivity GaSb. The possibility of lithium diffusion has been considered,²³ but with material grown from stoichiometric melts it gave resistivities only high enough not to cause masking of the phonon peaks, but not high enough for laser window applications.

The casting technique used for GaAs should be suitable for the production of relatively low cost 3" diameter windows, and could be applied to sizes up to 12" diameter. It is hoped that further experimental and theoretical work will give fuller insight into the mechanism causing the additional optical absorption in high resistivity material.

7. ACKNOWLEDGMENTS

The author wishes to acknowledge the invaluable assistance rendered by R. K. Willardson and J. W. Wagner of this laboratory. Discussions held with V. O. Nicolai, R. Rudko, T. Deutsch and B. Emmons have proved useful. The mass spectrometric analyses were ably performed by E. Masumoto. The competent technical assistance of F. Hicklin, K. Schwartz and T. Tench is gratefully recognized.

8. REFERENCES

1. R. I. Rudko and F. A. Horrigan, AD 693 311 (September, 1969).
2. F. Horrigan, C. Klein, R. Rudko and D. Wilson, Microwaves, p. 68 (Jan. 1969).
3. R. Gremmelmaier, Z. Naturforsch. 11A, 511 (1956).
4. E. P. A. Metz, R. C. Miller and R. Mazelsky, J. Appl. Phys. 33, 2016 (1962).
5. J. B. Mullin, B. W. Straugham and W. S. Brickell, J. Phys. Chem. Solids 26, 782 (1965).
6. J. W. Wagner and R. K. Willardson, Trans. Met. Soc. AIME 242, 366 (1968).
7. G. R. Cronin and R. W. Haisty, J. Electrochem. Soc. 111, 874 (1964).
8. O. Madelung, "Physics of III-V Compounds," Wiley, New York, p. 263 (1964).
9. J. Blanc and L. R. Weisberg, Nature 192, 155 (1961).
10. W. E. Pfann, "Zone Melting," Wiley, New York, p. 11 (2nd ed., 1966).
11. R. K. Willardson and W. P. Allred, Proc. of First Intl. Symp. on GaAs at Reading, p. 35 (1966), (Inst. of Phys. and Phys. Soc , London, 1967).
12. W. DeVilbiss, Ph.D. Thesis, U. of Missouri, Columbia, (1968).
13. T. Inoue and M. Ohyama, Solid State Comm. 8, 1309 (1970).
14. F. J. Reid, R. D. Baxter and S. E. Miller, J. Electrochem. Soc. 113, 713 (1966).
15. R. K. Willardson, Ann. N. Y. Acad. Sci. 137, 49 (1966).
16. "Semiconductors and Semimetals," R. K. Willardson and A. C. Beer, Eds., Vol. 3, (Academic Press, New York, 1967).
17. W. Cochran, S. J. Fray, F. A. Johnson, J. E. Quarrington and N. Williams, J. Appl. Phys. 32, 2102 (1961).

18. S. D. Smith, R. E. V. Chaddock and A. R. Goodwin, Proc. Int. Conf. Semiconductors, Kyoto, p. 67 (Suppl. to J. Phys. Soc. Japan 21, 1966).
19. C. A. Klein and R. I. Rudko, Appl. Phys. Letters 13, 129 (1968).
20. V. O. Nicolai and G. W. Gottlieb, Tech. Rept. No. AFWL-TR-69-108, AD 859 306 (1969).
21. R. Weil, J. Appl. Phys. 41, 3012 (1970).
22. A. G. Thompson, Semi-Annual Report, Contract N00014-70-C-0132, AD 709 576.
23. See, e.g. Chapter 2 of Reference 16.

UNCLASSIFIED

Security Classification

DOCUMENT CONTROL DATA - R & D

(Security classification of title, body of abstract and indexing annotation must be entered when the overall report is classified)

1. ORIGINATING ACTIVITY (Corporate author) BELL & HOWELL COMPANY, ELECTRONIC MATERIALS DIVISION 360 Sierra Madre Villa Pasadena, California 91109		2a. REPORT SECURITY CLASSIFICATION UNCLASSIFIED	
3. REPORT TITLE DEVELOPMENT OF GaAs INFRARED WINDOW MATERIAL		2b. GROUP	
4. DESCRIPTIVE NOTES (Type of report and inclusive dates) Technical Summary Report, 1 December 1969 through 30 November 1970.			
5. AUTHOR(S) (First name, middle initial, last name) Alan G. Thompson			
6. REPORT DATE December 1970	7a. TOTAL NO. OF PAGES 44	7b. NO. OF REFS 40	
8a. CONTRACT OR GRANT NO. N00014-70-C-0132	8b. ORIGINATOR'S REPORT NUMBER(S) --		
b. PROJECT NO. DEFENDER	8c. OTHER REPORT NO(S) (Any other numbers that may be assigned this report) --		
c.			
d.			
10. DISTRIBUTION STATEMENT This document has been approved for public release and sale; its distribution is unlimited.			
11. SUPPLEMENTARY NOTES --		12. SPONSORING MILITARY ACTIVITY OFFICE OF NAVAL RESEARCH Physics Branch Arlington, Virginia 22217	
13. ABSTRACT The choice of a window material suitable for high power CO ₂ lasers emitting at 10.6 microns is discussed. Gallium arsenide was chosen as the primary candidate with gallium antimonide being the object of a subsidiary investigation. The preparation of GaAs is discussed at length. The physical, electrical and optical properties of GaAs are also discussed with particular reference to the high-resistivity form which is necessary to reduce free-carrier absorption at 10.6 microns to an acceptable level. The method used to measure the optical absorption coefficient is a calorimetric one making use of a low power CO ₂ laser. The variation of the optical absorption coefficient with impurities, different dopants and resistivity is examined. An attempt was made to prepare high-resistivity GaSb, but this work is not yet complete. The preparation of larger diameter windows is described, with 3" being shown to be attainable with present technology.			

DD FORM 1473

1 NOV 55

REPLACES DD FORM 1473, 1 JAN 54, WHICH IS OBSOLETE FOR ARMY USE.

UNCLASSIFIED
Security Classification

14. KEY WORDS	LINK A		LINK B		LINK C	
	ROLE	WT	ROLE	WT	ROLE	WT
Semiconductors						
III-V Compounds						
Crystal Growth						
Gallium Arsenide						
Gallium Antimonide						
Impurities						
Electrical Properties						
Optical Absorption						
Infrared Windows						
Carbon Dioxide Lasers						